Electrochemical Behavior and Redox-Dependent Disassembly of Gallic Acid/Fe^{III} Metal–Phenolic Networks

Pavel V. Cherepanov, [†] Md. Arifur Rahim, [†] Nadja Bertleff-Zieschang, [†] Md. Abu Sayeed, [‡] Anthony P. O'Mullane, [‡] Simon E. Moulton, [‡] and Frank Caruso*, [†]

[†]ARC Centre of Excellence in Convergent Bio-Nano Science and Technology, and the Department of Chemical Engineering, The University of Melbourne, Parkville, Victoria 3010, Australia

[‡] ARC Centre of Excellence for Electromaterials Science, Faculty of Science, Engineering and Technology, Swinburne University of Technology, Hawthorn, Victoria 3122, Australia

[‡] School of Chemistry, Physics and Mechanical Engineering, Queensland University of Technology (QUT), Brisbane, Queensland 4001, Australia

ABSTRACT

Upon its recent introduction, a versatile class of organic-inorganic hybrid systems known as metal-phenolic networks (MPNs) has been steadily growing its potential for applications in various fields such as catalysis, bio-imaging, and drug-delivery. Many of these applications involve the processes of mediation, disassembly, and/or release, which often rely on redox-dependent interactions. Self-assembled MPNs, possessing metal-coordinated structures, may potentially serve as redox responsive platforms, offering an additional tool of control for triggered disassembly or drug release. Therefore, a comprehensive study of MPN's reduction/oxidation behaviour for evaluation of its redox responsiveness, specific conditions for disassembly and comments on the kinetics of metal ion release is necessary. Starting with a gallic acid – iron (GA/Fe^{III}) system as a simple MPN representative, we carried out electrochemical characterisation to provide valuable fundamental insights into the redox behavior of these networks. We demonstrate that GA/Fe^{III} is redox active, evaluate its electrochemical reversibility, identify the oxidation state of the redox active species, and provide information regarding stability towards reductive stimuli and specific redox conditions for Fe^{III} "on-off" or continuous release. Overall, through studying the redox

properties of GA/Fe^{III} film, we advance the understanding of multi-functional iron containing MPNs platforms for the wide range of biologically relevant applications.

INTRODUCTION

Functional hierarchical materials fabricated using coordination-driven self-assembly are of importance in diverse fields of materials science [1-4]. Among these, is the recently reported versatile class of organic-inorganic hybrid systems known as metal-phenolic networks (MPNs) [5]. Typically, MPNs are formed using either synthetic or naturally abundant phenolic compounds, bearing catechol or galloyl groups, and transition metals as structural motifs [5-9]. The formation of MPNs on a solid substrate involves the interfacial assembly of strongly coordinated metal-phenolic complexes resulting in stable, surface-confined, amorphous films. Advancing from the initial use of tannic acid (TA) as a macromolecular polyphenolic ligand [5, 7], the MPN assembly process has been observed to be more generic in nature and applicable to simpler phenolic moieties such as gallic acid (GA), pyrogallol (PG), and pyrocatechol (PC). MPN films formed by these small phenolic ligands and Fe^{III} have provided valuable insights into structural requirements for the assembly process and details on coordination chemistry of the resulting networks [9]. Moreover, these findings have guided the design of iron-containing MPNs from other small biologically functional ligands such as quercetin and myricetin [10].

To date, MPNs have already shown potential applications in various fields such as catalysis, separation, bio-imaging and drug-delivery [7, 11-13]. Though progress has been made in understanding the assembly, structure, and physicochemical properties [5, 7, 9, 14] the electrochemical nature of MPNs has rarely been investigated [15]. In general, ortho-dihydroxybenzenes are known to be redox active in their non-coordinated form as well as coordinated in discrete metal complexes [16-18]. Thus, it can be expected that the coordinated structures of amorphous MPNs will respond to electrochemical stimuli and that such a response will add to our current understanding of the nature of the coordination network. In particular, thorough electrochemical analysis of MPN systems might provide details on characteristics such as red-ox activity and its reversibility, the oxidation state of the redox active species, and specific conditions for controlled disassembly. Overall, understanding of MPN's reduction/oxidation properties may provide valuable fundamental insights for the future design of electrochemical actuators for biologically relevant and wide-ranging applications in medicine, e.g., controlled drug release [19-22]. The applicability of

MPNs can be extended even further owning to their structural features. For example, precise control of iron-containing MPN disassembly might be useful in the environments such as soils, fresh and marine waters where bioavailability of iron is compromised due to its poor solubility. Therefore, MPNs also have the potential to serve as an iron supplement controlling/regulating platforms for agri/aquaculture, and marine science [23-25].

Herein, we focused on the electrochemical behaviour of a MPN system prepared using a simple and naturally abundant phenolic ligand of GA and Fe^{III} as a metal cross-linker. Electrochemical characterization was performed by employing cyclic voltammetry and chronoamperometry techniques under both static and dynamic conditions. The as-prepared GA/Fe^{III} film was found to be redox responsive and its electrochemical response was correlated to the specific coordination interactions. We also analysed the reversibility of the electrochemical response and provide details regarding the nature of the redox active species within the GA/Fe^{III} network. Additionally, we report on the possible release of Fe^{III} from the network triggered by electrochemical stimuli, and demonstrate the specific redox conditions for the continuous disassembly of a GA/Fe^{III} film.

RESULTS AND DISSCUSSION

GA/Fe^{III} capsules were prepared utilizing a coordination-driven self-assembly approach according to our previous report [9]. In brief, the ~ 3.2 µm size polystyrene (PS) particles used as a template were mixed with an aqueous solution of gallic acid (GA) followed by addition of an aqueous solution of iron (III) chloride in a stoichiometric ratio of 1:1 and, upon the adjustment of the pH to ~3.8, the PS cores were dissolved using THF (the full characterization has been reported elsewhere [9]). To study their electrochemical behaviour, freshly prepared GA/Fe^{III} capsules were resuspended in an ethanol/nafion solution which was drop-cast on a glassy carbon electrode (GCE) and air dried (see SI for details). It is important to note that we used the capsules throughout this study for two reasons: i) the electrochemical behaviour of planar and colloidal films has been demonstrated to be identical, [26-28] ii) colloidal MPN films (i.e., capsules) can be produced with high degree of precision and homogenous film thickness, which is difficult to achieve for planar films since it requires multiple cycles to obtain the complete coverage of planar substrates [5]. **Figure 1a** schematically shows the synthesis of GA/Fe^{III} capsules and their preparation for electrochemical studies. A cyclic voltammogram (CV) for the GA/Fe^{III} system was recorded

in the potential range of -500 mV to +900 mV and is shown in **Figure 1b**. It is noteworthy to mention that the potential window was chosen to exclude/reduce any possible competitive processes of hydrogen and oxygen evolution [29, 30] that might affect the electrochemical data evaluation, which, for the majority of studied materials occur outside of this selected range. As it can be seen from the recorded CV, the GA/Fe^{III} network exhibits a well pronounced redox response, with distinct oxidation and reduction processes as compared to a CV recorded at a bare GCE (**Figure 1b**, black dotted line). In the forward scan from 0 to +900 mV, the oxidation of GA/Fe^{III} begins at a low potential of +80 mV and continues until it reaches the observed current density value of ~0.11 mA/cm^2. During the reverse scan from +900 mV to -500 mV a reduction peak at +80 mV with a much lower magnitude of ca. -0.02 mA/cm^2 appeared. The observed (about 5-fold) difference in absolute values recorded for the oxidation and reduction processes (0.11 mA/cm^2 vs. -0.02 mA/cm^2) might correspond to the following scenarios. Thus, during the initial CV cycle, at a given scan rate and the chosen potential window range, the redox active species present in GA/Fe^{III} network; (i) are of the same nature, though, differ in terms of reduction and oxidation kinetics; or (ii) are of a different nature.

To reveal the origin of the GA/Fe^{III} network redox responsiveness, we recorded a CV for a GA solution (**Figure 2a**) which was used as a reference. For GA, we observed two separate oxidation peaks at +350 mV and +650 mV. The first peak at a lower potential appears due to the oxidation of the catechol group present in GA corresponding to a quinone motif, whereas the second peak (at higher potential) is the oxidation of single hydroxyl groups. This observation agrees well with previously reported electrochemical data for GA and similar phenolic compounds [16, 31]. It is also important to note that, based on the oxidation peak position and the corresponding magnitude of the current, oxidation of the GA catechol group to quinone is the dominant process. Moreover, oxidation of GA as a whole is an irreversible process and indeed, we did not observe any related reduction peaks (**Figure 2a**). Therefore, this observation indicates that the oxidation response of this iron-coordinated network, upon the first forward scan, primarily originates from the phenolic ligand itself. This observation can be additionally supported by the fact that GA/Fe^{III} capsules contain iron in the oxidation state 3+ [9, 32] which is highly unlikely to further oxidize.

Furthermore, knowing that the phenolic ligand is irreversibly oxidized, we then suggest that the peak upon the reverse scan for the GA/Fe^{III} network must originate from the Fe^{III} to Fe^{II}

reduction process. To investigate this further, we recorded a CV for GA/Fe^{III} with a starting potential of +100 mV and ran it to a lower limit of -500 mV first, followed by an additional complete CV cycle **(Figure 2b**). The starting potential of +100 mV was selected to avoid oxidation of the phenolic ligand within the iron-coordinated network. Surprisingly, we did not observe any reduction peak despite the presence of Fe^{III} within the network which can potentially be reduced to Fe^{II}. We assume that Fe^{III} is strongly coordinated to the phenolic ligand in the GA/Fe^{III} network (**Figure 2c**), and therefore, is irresponsive to reductive stimuli in the chosen potential scan range. Interestingly, the reduction peak only appears upon completion of the consecutive oxidation scan. This finding can be explained by the irreversible oxidation of the catechol groups to a quinone at the more positive potential as determined for the free ligand. Even after oxidation the Fe^{III} must still be coordinated to the quinone groups (**Figure 2d**), but significantly weaker as compared to an iron-catechol coordination complex [33] thereby making the metal ion available for reduction. Overall, based on the obtained electrochemical data, we confirm that the redox active species present in a GA/Fe^{III} network are indeed of a different nature with the gallic acid ligand being oxidized creating a weaker Fe^{III}-ligand interaction allowing the Fe^{III} ions to be reduced during the first complete CV scan.

To evaluate the redox behaviour of the GA/Fe^{III} system further, especially upon irreversible oxidation of the phenolic ligand, we recorded 5 consecutive CVs in the potential range of -500 mV and +900 mV. As it can be seen from **Figure 3a**, the redox response of the GA/Fe^{III} network is of a quasi-reversible character; i.e. oxidation and reduction peaks are clearly identifiable for each cycle, though, with a noticeable decrease in the current magnitude compared to the first cycle (Figure 2b). The abrupt current drop, especially for the oxidation peak, is observed between the 1^{st} and 2^{nd} as well as 2^{nd} and 3^{rd} cycles, after which it stabilizes; whereby the 4^{th} and 5^{th} cycles are very similar in magnitude. We attribute the oxidation peak current decrease between the 1^{st} and 2^{nd} cycles to the irreversible oxidation of the phenolic ligand. The oxidation peak that is seen on the second CV most likely occurs due to both; (i) phenolic ligand oxidation of an intact portion of the GA/Fe^{III} network and (ii) oxidation of Fe^{II} back to Fe^{III} after its reduction during the first CV scan. A similar scenario is valid for all consecutive CV cycles until oxidation of the ligand is complete and only the quasi-reversible (the peak to peak separation is greater than 59 mV) oxidation/reduction of Fe^{II}/Fe^{III}-quinone complex is observed (**Figure 3b**). Assuming that the last statement is valid for the 5^{th} CV cycle, we made an attempt to estimate the oxidized portion of the phenolic

ligand upon completion of each CV cycle. **Figure 3b** shows the remaining percentage of the oxidation current with respect to the cycle number. The current exponentially decays to about 20 % of its original value which can be attributed to the quasi-reversible Fe^{II} to Fe^{III} oxidation response during each cycle, except for the first cycle as noted earlier. Therefore, for a given amount of GA/Fe^{III} sample ~80 % of the phenolic ligand is irreversibly oxidized after completion of the first CV cycle with the remaining 20 % of the ligand being oxidized over the next three cycles. It is important to note, that the reduction peak current is also decreasing after completion of a few CV scans. Although the decrease in magnitude is not as drastic as the oxidation process, it is possibly due to partial loss/release of the metal ion from the GA/Fe^{III} network during the imposed electrochemical stimulus.

To support the proposed idea that iron ions are being released from the GA/Fe^{III} network during its oxidation, we modified the experimental setup for further electrochemical characterization. More precisely, we replaced a conventional GCE used under static conditions, with a rotating ring-disk electrode (RRDE) on which the GA/Fe^{III} capsule ethanol/nafion suspension was drop cast onto the disc portion of the electrode and air-dried (**Figure 4a**). The main advantage of using a RRDE is the ability of employing various electrochemical techniques simultaneously. Thus, the glassy carbon disk with drop casted GA/Fe^{III} capsules was subject to a CV scan in the potential region of -450 mV to +700 mV, while the gold ring was kept at a constant and sufficient potential of -450 mV for the reduction of Fe^{III} ions that may be liberated into solution.

We hypothesise that upon oxidation of the GA/Fe^{III} network, weakly coordinated metal ions in the Fe^{III} - quinone complex due to physical disturbance caused by electrode rotation (1000 rpm) would be swept away from the network and driven to the gold ring electrode where it would be reduced to Fe^{II}. As can be seen from the recorded chronoamperometric (CA) profile at the gold ring electrode as shown in **Figure 4b**, the current increases with time (during the forward CV scan) directly proving Fe^{III} reduction occurs which originates from the gradually oxidizing GA/Fe^{III} network. The reduction current on the ring is measured up until almost the end of the reverse CV scan where the supply of Fe^{III} ion is decreasing. At this point, the Fe^{III} ion is simply being reduced within the GA/Fe^{III} network at the disc electrode resulting in a lower amount of Fe^{III} ion available for reduction at the ring electrode which is reflected in current drop in the recorded CA. At the beginning of the second CV scan the supply of Fe^{III} ion is re-established (upon further oxidation of the phenolic ligand and the newly formed Fe^{II}

which becomes oxidised) and the process repeats itself (**Figure 4c**). We continued recording CA experiments at the ring electrode while simultaneously running up to 20 consecutive CV cycles to obtain information regarding the longevity of GA/Fe^{III} capsules under repetitive oxidation/reduction conditions. We observed a repetitive local "on-off" character of Fe^{III} release during the reductive/oxidative stimuli which induced the disassembly of the metal phenolic network. Overall, the largest amount of iron was released after ~ 35 min which was completely spent after 80 min at the given electrochemical conditions of potential scan range and sweep rate. Furthermore, to test whether continuous Fe^{III} ion release from the GA/Fe^{III} network could be achieved, we ran CV scans in a more limited potential window range of +150 mV to +700 mV to avoid the reduction of released Fe^{III} in solution back to Fe^{II}. The phenolic ligand is expected to be constantly oxidizing on the forward cycle and forming a weaker Fe^{III}-quinone complex, from which Fe^{III} ions should be released and subsequently monitored at the ring electrode. As in previous case, a constant potential of -450 mV was applied to the gold ring for recording the CA for 20 CV cycles at the disk electrode (**Figure 4d**). As expected, we did not observe any disruption or "on-off" type behaviour in Fe^{III} ion release on the recorded CA profile during repetitive cycling, as in case with the broader potential range that would encompass reduction of Fe^{III} ions. Therefore, by avoiding Fe^{III} ion reduction in the network while constantly oxidizing the ligand, the continuous release of iron ions from the GA/Fe^{III} network can be achieved.

CONCLUSIONS

In summary, we have demonstrated that a MPN film prepared from a small phenolic ligand of GA and Fe^{III} as a metal cross-linker is an electrochemically active system and its redox response is of a quasi-reversible character. Our results suggest that the initial redox responses of the GA/Fe^{III} network originate from the irreversible oxidation of the ligand as well as the quasi-reversible reduction of the metal ion. Nevertheless, in chosen potential regions the MPN network is unresponsive to reductive stimuli unless oxidized beforehand. More specifically, the strong Fe^{III} – gallic acid interaction can be weakened during ligand oxidation (~80% upon the first CV cycle) which leads to the formation of a less stable coordination complex. Finally, we proved qualitatively that the release of Fe^{III} from the network upon inducing the electrochemical stimuli can be achieved. It was also demonstrated that the specific redox conditions for its' "on-off" or continuous supplement of ions to the aqueous environment could be controlled. Overall, our results unravel valuable fundamental insights

for the future design of multi-functional MPN platforms for various biologically relevant applications and may have implications for drug delivery whereby an oxidising environment of sufficient redox potential will be required to weaken the phenolic network. We are currently extending our investigation to similar MPN systems including the use of other simple phenolic ligands and different metal ions.

EXPERIMENTAL

Materials. Gallic acid (GA, 97.5%), iron(III) chloride hexahydrate ($FeCl_3 \cdot 6H_2O$), sodium hydroxide (NaOH), sodium sulfate (Na_2SO_4) were purchased from Sigma-Aldrich and used as received. Polystyrene (PS) particles (D = 3.20 ± 0.07 μm) were purchased from Microparticles GmbH. Tetrahydrofuran (THF) was purchased from Chem Supply. High-purity (Milli-Q) water with a resistivity of 18.2 MΩ cm was obtained from an inline Millipore RiOs/Origin water purification system.

GA/ Fe^{III} Film Formation on Particulate Substrates. The standard protocol is described as follows. 50 μL of polystyrene (PS, D = 3.20 ± 0.07 μm, 10% (w/w) water suspension) particles was first washed twice with Milli-Q water. Then, 400 μL of the ligand (GA) solution (15 mM) was added to the PS particles and vortexed for 10 s. 200 μL of $FeCl_3 \cdot 6H_2O$ (30 mM) solution was then added and quickly vortexed for 3−4 s. Subsequently, the mixture pH was raised by addition of 20 μL of 0.5 M NaOH solution, followed by vortexing for 1 min; the final pH values of the mixture was ~3.8. Unreacted supernatant was removed by centrifugation (1700g, 1 min) followed by four washing steps in Milli-Q water. Dissolution of the PS cores was accomplished by washing the pellets with THF three times (1900g, 1 min). The obtained hollow capsules were washed twice (2000g, 3 min) with Milli-Q water and finally resuspended in 400 μL of Milli-Q water for characterization.

Characterization.

Differential interference contrast (DIC) microscopy images were taken with an inverted Olympus IX71 microscope.

Electrochemical experiments in static conditions were performed using a MM510 Potentiostat/Galvanostat (MMates, Italy). A standard three-electrode electrochemical cell was used to record cyclic voltammograms where glassy carbon electrode (GCE, 3mm diameter) served as a working, Pt-wire as a counter, and Ag/AgCl(KCl) as a reference electrode respectively.

Electrochemical experiments under dynamic conditions were performed using an Autolab Bipotentiostat/Galvanostat (BioLogic VSP workstation). A similar three-electrode electrochemical cell setup was used to record cyclic voltammograms and chronoamperograms with the exception of using a rotating ring-disk (BAS) as a working electrode (RRDE, glassy carbon disk – 4 mm diameter, gold ring width – 2 mm, the gap between outer circle of the disk and inner circle of the ring – 1 mm). The rotating speed was set to 1000 rpm.

For all electrochemical measurements 1M Na_2SO_4 aqueous solution was used as a supporting electrolyte. The supporting electrolyte was deaerated by purging nitrogen for 30 min before each measurement. The total amount of freshly prepared GA/Fe^{III} capsules yielded upon described experimental procedure (~ 2×10^6) was resuspended in 2.5 µL/ 25 µL Nafion/Ethanol solution. 10 µL of the resulting GA/Fe^{III} capsule suspension were drop cast on GCE or RRDE and air-dried. Before each drop-casting procedure, both GCE and RRDE were thoroughly polished using alumina polishing kit and washed with ethanol.

Cyclic voltammograms on the GCE were recorded in the potential region of -0.5 V to +0.9 V for the GA/Fe^{III} systems and -0.9 V to +0.9 V for the 15mM gallic acid solution. In each case, the scan rate was 5 mV/s.

Cyclic voltammograms for the GA/Fe^{III} system on the RRDE were recorded in the potential region of -0.45 V to +0.7 V and +0.15 V to +0.7 V. In each case, the scan rate was 10 mV/s. Chronoamperograms were recorded at the gold ring electrode at a constant potential of -0.45 V.

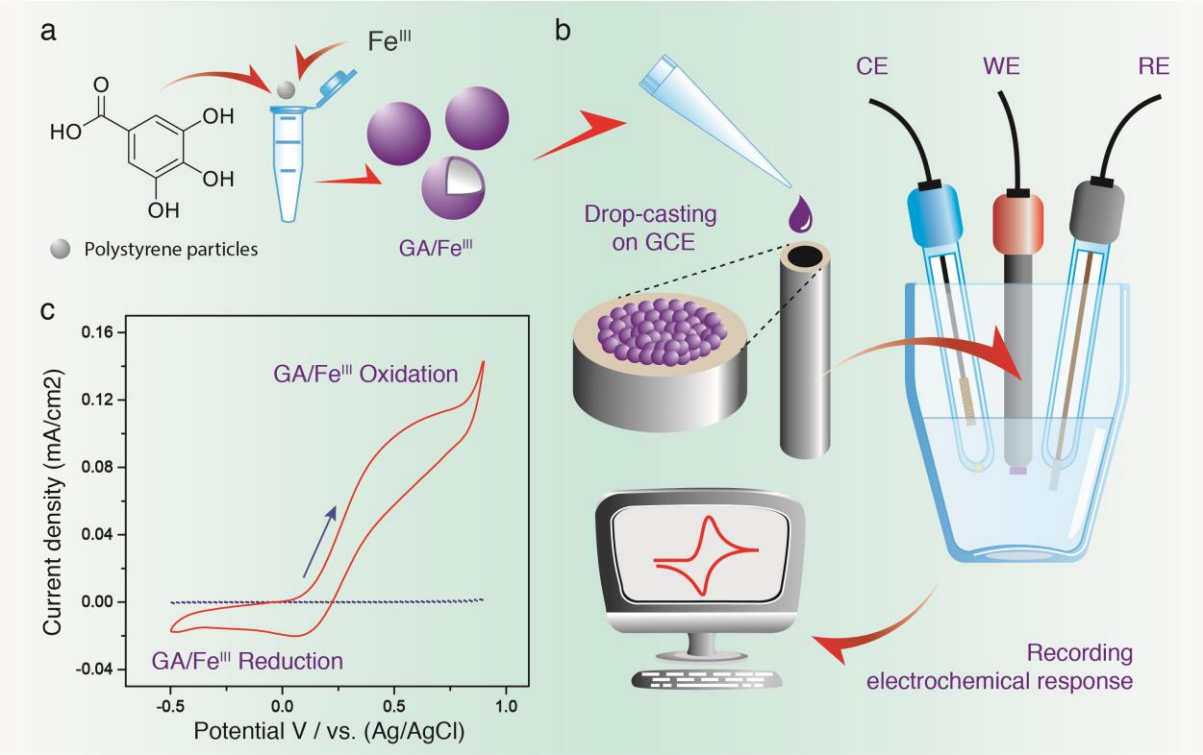

Figure 1. Schematic representation of the GA/Fe^{III} network fabrication (a) and an overview of the experimental setup for their electrochemical characterization (b). Recorded under static conditions, a cyclic voltammogram for the GA/Fe^{III} network in an aqueous solution of 1M Na_2SO_4 (c). Dotted line in (c) represents bare glassy carbon electrode as a reference. The arrow indicates direction of CV scan. The scan rate is 5 mV/s.

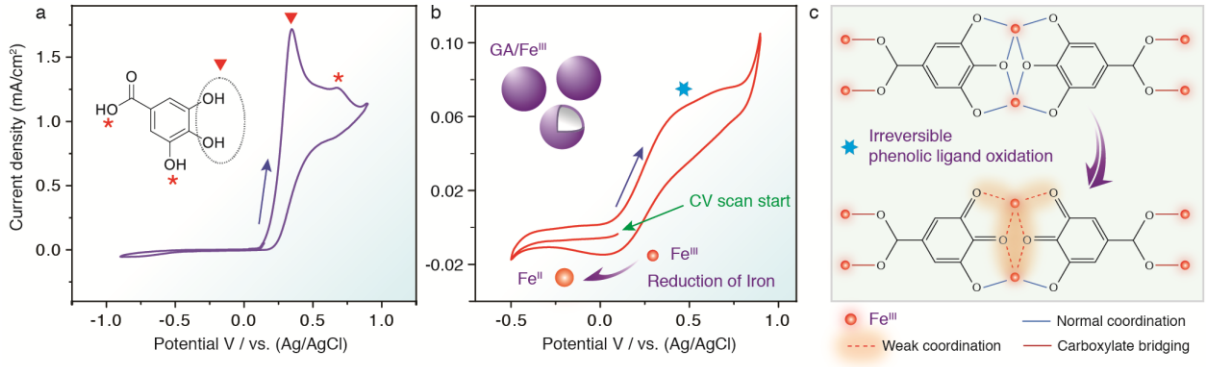

Figure 2. Recorded under static conditions, a cyclic voltammogram for a 15 mM GA aqueous solution at a bare GCE (a) and the GA/Fe^{III} network (b). The CV in (b) was originally swept from +100 mV to -500 mV followed by a complete cycle. The blue arrows in (a) and (b) indicate the direction of the scan. The green arrow in (b) shows the start of the scan. The scan rate is 5 mV/s. Schematic representation of possible phenolic ligand oxidation assuming irreversible oxidation of the catechol to the quinone dominates the process (c).

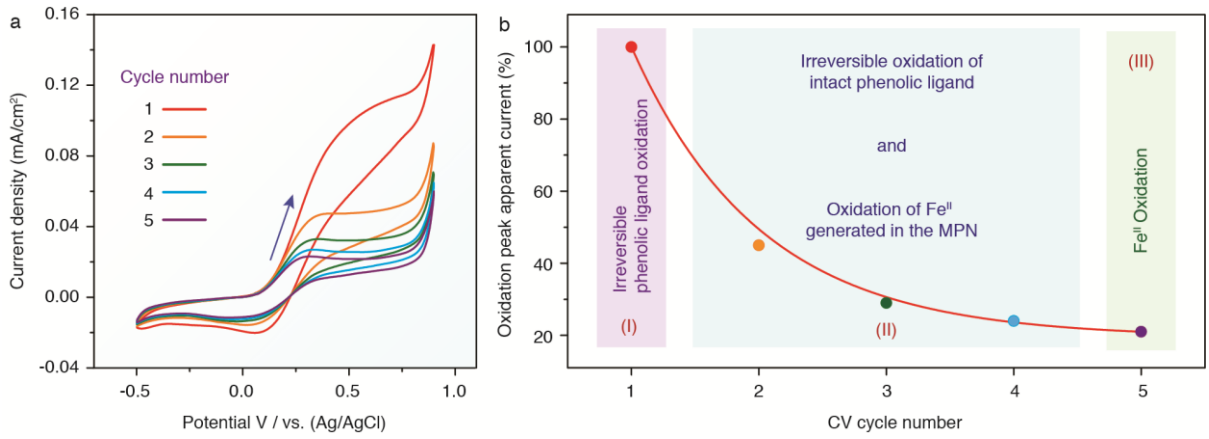

Figure 3. Recorded under static conditions, repetitive cyclic voltammograms for the GA/Fe^{III} network (a). The plot (b) shows the remaining percentage of the oxidation peak current in (a) as a function of the number of CV cycles. The arrow in (a) indicates the direction of the scan. The scan rate is 5 mV/s.

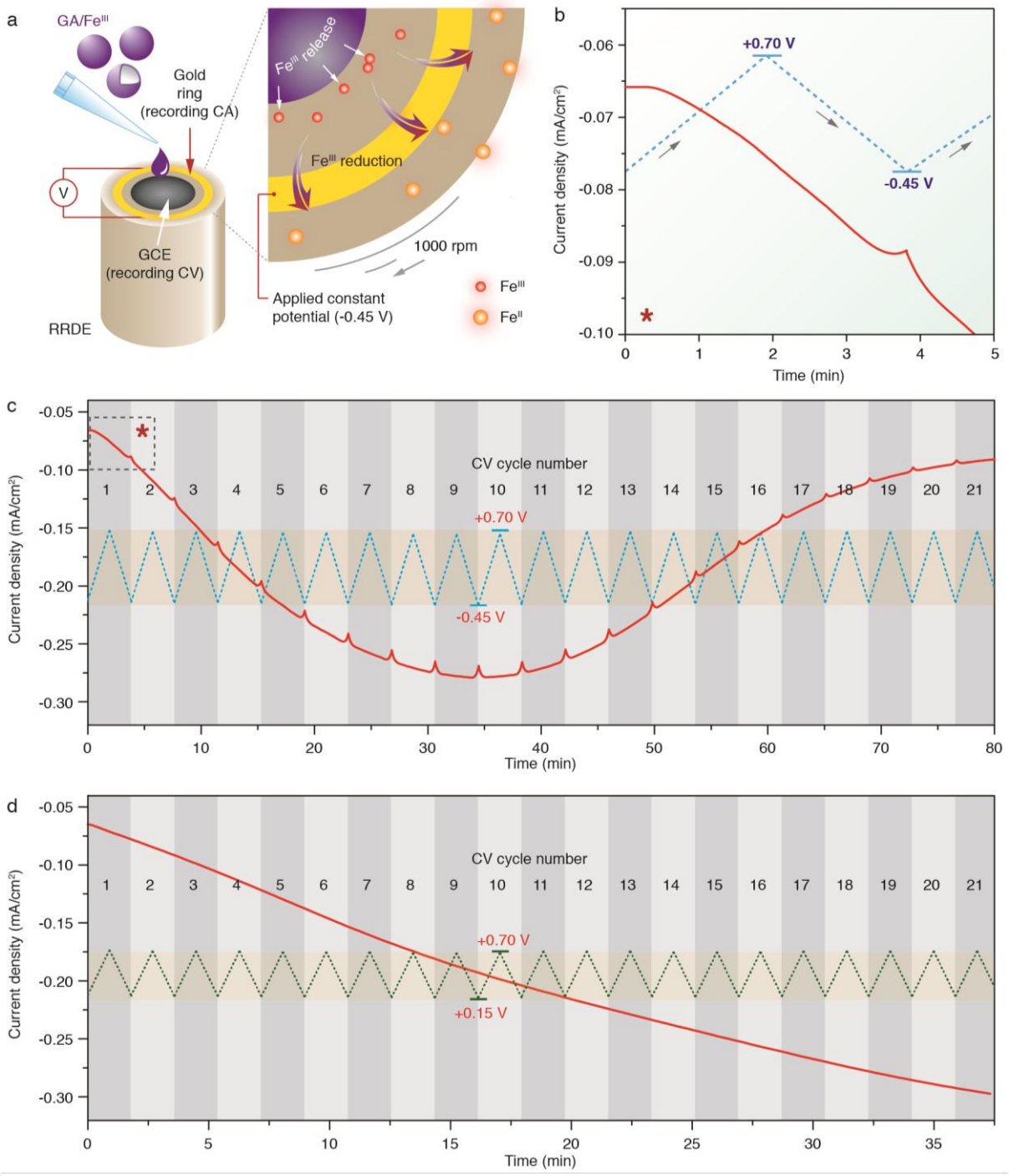

Figure 4. Schematic representation of Fe^{III} release from the GA/Fe^{III} network drop-casted on a glassy carbon disk and its reduction to Fe^{II} at the gold ring of a rotating ring-disk electrode (a). Chronoamperogram recorded at the gold ring during the first CV cycle of the GA/Fe^{III} network in the potential region of -450 mV to +700 mV (b). Extended CA profiles during 21 consecutive CV cycles of the GA/Fe^{III} network in the potential region of -450 mV to +700 mV (c) and +150 mV to +700 mV (d). The rotating speed is 1000 rpm. The scan rate is 10 mV/s. Applied constant potential of the gold ring is -450 mV.

[1] Y. Cui, B. Li, H. He, W. Zhou, B. Chen, G. Qian, Metal–Organic Frameworks as Platforms for Functional Materials, Accounts of Chemical Research, 49 (2016) 483-493.
[2] M.L. Foo, R. Matsuda, S. Kitagawa, Functional Hybrid Porous Coordination Polymers, Chemistry of Materials, 26 (2014) 310-322.
[3] A. Kaushik, R. Kumar, S.K. Arya, M. Nair, B.D. Malhotra, S. Bhansali, Organic–Inorganic Hybrid Nanocomposite-Based Gas Sensors for Environmental Monitoring, Chemical Reviews, 115 (2015) 4571-4606.
[4] J. Zhang, C.-Y. Su, Metal-organic gels: From discrete metallogelators to coordination polymers, Coordination Chemistry Reviews, 257 (2013) 1373-1408.
[5] H. Ejima, J.J. Richardson, K. Liang, J.P. Best, M.P. van Koeverden, G.K. Such, J. Cui, F. Caruso, One-Step Assembly of Coordination Complexes for Versatile Film and Particle Engineering, Science, 341 (2013) 154.
[6] H. Ejima, J.J. Richardson, F. Caruso, Phenolic film engineering for template-mediated microcapsule preparation, Polym. J., 46 (2014) 452-459.
[7] J. Guo, Y. Ping, H. Ejima, K. Alt, M. Meissner, J.J. Richardson, Y. Yan, K. Peter, D. von Elverfeldt, C.E. Hagemeyer, F. Caruso, Engineering Multifunctional Capsules through the Assembly of Metal–Phenolic Networks, Angewandte Chemie International Edition, 53 (2014) 5546-5551.
[8] M.A. Rahim, M. Björnmalm, T. Suma, M. Faria, Y. Ju, K. Kempe, M. Müllner, H. Ejima, A.D. Stickland, F. Caruso, Metal–Phenolic Supramolecular Gelation, Angewandte Chemie International Edition, 55 (2016) 13803-13807.
[9] M.A. Rahim, K. Kempe, M. Müllner, H. Ejima, Y. Ju, M.P. van Koeverden, T. Suma, J.A. Braunger, M.G. Leeming, B.F. Abrahams, F. Caruso, Surface-Confined Amorphous Films from Metal-Coordinated Simple Phenolic Ligands, Chemistry of Materials, 27 (2015) 5825-5832.
[10] N. Bertleff-Zieschang, M.A. Rahim, Y. Ju, J.A. Braunger, T. Suma, Y. Dai, S. Pan, F. Cavalieri, F. Caruso, Biofunctional metal-phenolic films from dietary flavonoids, Chemical Communications, 53 (2017) 1068-1071.
[11] P. Han, J. Shi, T. Nie, S. Zhang, X. Wang, P. Yang, H. Wu, Z. Jiang, Conferring Natural-Derived Porous Microspheres with Surface Multifunctionality through Facile Coordination-Enabled Self-Assembly Process, ACS Appl. Mater. Interfaces, 8 (2016) 8076-8085.
[12] Y. Ju, Q. Dai, J. Cui, Y. Dai, T. Suma, J.J. Richardson, F. Caruso, Improving Targeting of Metal–Phenolic Capsules by the Presence of Protein Coronas, ACS Appl. Mater. Interfaces, 8 (2016) 22914-22922.
[13] H. Liang, J. Li, Y. He, W. Xu, S. Liu, Y. Li, Y. Chen, B. Li, Engineering Multifunctional Films Based on Metal-Phenolic Networks for Rational pH-Responsive Delivery and Cell Imaging, ACS Biomater. Sci. Eng., 2 (2016) 317-325.
[14] H. Liang, B. Zhou, J. Li, W. Xu, S. Liu, Y. Li, Y. Chen, B. Li, Supramolecular design of coordination bonding architecture on zein nanoparticles for pH-responsive anticancer drug delivery, Colloids and Surfaces B: Biointerfaces, 136 (2015) 1224-1233.
[15] C. Meyer, F. Ponzio, E. Mathieu, V. Ball, Kinetics of deposition and stability of pyrocatechol –FeIII coordinated films, Materials Science and Engineering: C.
[16] R. Abdel-Hamid, E.F. Newair, Electrochemical behavior of antioxidants: I. Mechanistic study on electrochemical oxidation of gallic acid in aqueous solutions at glassy-carbon electrode, Journal of Electroanalytical Chemistry, 657 (2011) 107-112.

[17] C.H. Hung, W.T. Chang, W.Y. Su, S.H. Cheng, Electrochemical Determination of Pyrogallol at Conducting Poly(3,4-ethylenedioxythiophene) Film-Modified Screen-Printed Carbon Electrodes, Electroanalysis, 26 (2014) 2237-2243.
[18] D. Nematollahi, M. Rafiee, Electrochemical oxidation of catechols in the presence of acetylacetone, Journal of Electroanalytical Chemistry, 566 (2004) 31-37.
[19] A. Anderson, J. Davis, Electrochemical Actuators: Controlled Drug Release Strategies for use in Micro Devices, Electroanalysis, 27 (2015) 872-878.
[20] H. Lee, T.K. Choi, Y.B. Lee, H.R. Cho, R. Ghaffari, L. Wang, H.J. Choi, T.D. Chung, N. Lu, T. Hyeon, S.H. Choi, D.-H. Kim, A graphene-based electrochemical device with thermoresponsive microneedles for diabetes monitoring and therapy, Nat Nano, 11 (2016) 566-572.
[21] D. Svirskis, J. Travas-Sejdic, A. Rodgers, S. Garg, Electrochemically controlled drug delivery based on intrinsically conducting polymers, Journal of Controlled Release, 146 (2010) 6-15.
[22] S. Szunerits, F. Teodorescu, R. Boukherroub, Electrochemically triggered release of drugs, European Polymer Journal, 83 (2016) 467-477.
[23] M. Balhara, R. Chaudhary, S. Ruhil, B. Singh, N. Dahiya, V.S. Parmar, P.K. Jaiwal, A.K. Chhillar, Siderophores; iron scavengers: the novel & promising targets for pathogen specific antifungal therapy, Expert Opinion on Therapeutic Targets, 20 (2016) 1477-1489.
[24] D.A. Hutchins, A.E. Witter, A. Butler, G.W. Luther, Competition among marine phytoplankton for different chelated iron species, Nature, 400 (1999) 858-861.
[25] B.R. Wilson, A.R. Bogdan, M. Miyazawa, K. Hashimoto, Y. Tsuji, Siderophores in Iron Metabolism: From Mechanism to Therapy Potential, Trends in Molecular Medicine, 22 (2016) 1077-1090.
[26] J. Cui, Y. Liu, J. Hao, Multiwalled Carbon-Nanotube-Embedded Microcapsules and Their Electrochemical Behavior, The Journal of Physical Chemistry C, 113 (2009) 3967-3972.
[27] D.G. Shchukin, K. Köhler, H. Möhwald, Microcontainers with Electrochemically Reversible Permeability, Journal of the American Chemical Society, 128 (2006) 4560-4561.
[28] S. Zheng, C. Tao, Q. He, H. Zhu, J. Li, Self-assembly and Characterization of Polypyrrole and Polyallylamine Multilayer Films and Hollow Shells, Chemistry of Materials, 16 (2004) 3677-3681.
[29] P.C. Chen, Y.M. Chang, P.W. Wu, Y.F. Chiu, Fabrication of Ni nanowires for hydrogen evolution reaction in a neutral electrolyte, International Journal of Hydrogen Energy, 34 (2009) 6596-6602.
[30] P.V. Cherepanov, I. Melnyk, E.V. Skorb, P. Fratzl, E. Zolotoyabko, N. Dubrovinskaia, L. Dubrovinsky, Y.S. Avadhut, J. Senker, L. Leppert, S. Kummel, D.V. Andreeva, The use of ultrasonic cavitation for near-surface structuring of robust and low-cost AlNi catalysts for hydrogen production, Green Chemistry, 17 (2015) 2745-2749.
[31] A.M.O. Brett, M.E. Ghica, Electrochemical oxidation of quercetin, Electroanalysis, 15 (2003) 1745-1750.
[32] E. Nkhili, M. Loonis, S. Mihai, H. El Hajji, O. Dangles, Reactivity of food phenols with iron and copper ions: binding, dioxygen activation and oxidation mechanisms, Food & Function, 5 (2014) 1186-1202.
[33] R.C. Hider, Z.D. Liu, H.H. Khodr, Metal chelation of polyphenols, Methods in Enzymology, 335 (2001) 190-203.